Electrochemical characteristics and application of thiophenol self-assembling monolayer modified gold electrode*

CAI Chenxin (蔡称心), JU Huangxian (鞠熀先) and CHEN Hongyuan (陈洪渊)**

(Department of Chemistry, Nanjing University, Nanjing 210093, China)

Received January 20, 1995

Keywords: monomolecular layer, chemically modified electrode, A.C. impedance, microelectrode assembly, thiophenol.

The modification of electrode involves the attachment of chemical substances to the surfaces by physical adsorption, chemical bonding or polymer coating. The modified electrodes can thereby exhibit properties related to those of the modifying substances. It is quite clear that in order to perform increasingly complicated and demanded tasks using chemically modified electrodes, complex molecular structure must be constructed with a high degree of control over the design and structure of the systems. The merits of organized monolayer techniques for electrode surface modification have been recongnized recently using both the Langmuir-Blodgett (LB) technique and self-assembling monolayer. Such a monolayer provides a means of controlling the chemical structure at the molecular level on the surface of the electrodes. The former researches mainly deal with the self-assembling monolayer of alkanethiols on the gold surface, which was formed through Au—S bond[1]. In this note, we studied the electrochemical characteristics of the monolayer of thiophenol, an aromatic thiol, modified gold electrode (defined as Au/TP) which was prepared by self-assembly technique. The experimental results show that the Au/TP electrode behaves as a microelectrode assembly. In this note we also discussed the application of this monolayers-based microelectrode assembly to the investigation of the complicated electrochemical reaction mechanism and the determination of the heterogeneous electron transfer rate constant for fast redox couples, such as $Fe(CN)_6^{4-/3-}$.

1 Experimental

All chemicals were of analytical grade. Thiophenol (TP) was used as received without further purification. Twice-distilled water was used in all experiments. A PAR M270 electrochemistry system (EG&G, PAR) was used for cyclic voltammetric measurements and

* Project supported by the National Natural Science Foundation of China.

** To whom correspondence should be addressed.

an M273 potentiostat and PAR 5028 locked phase amplifier with an M388 A.C. impedance system were used for A.C. impedance measurements. Measurements were carried out with an amplitude of 5 mV (100 kHz—6.3 Hz) and 10 mV. The A.C. impedance measurements were carried out with an amplitude of 5 mV (100 kHz~6.3 Hz) and 10 mV(0.1 Hz—6.3 Hz). The RA-FTIR of Au/TP electrode was obtained by a 170SX-FTIR spectrometer (Nicolet, USA).

A three-electrode system with a platinum wire as the counter electrode, a saturated calomel electrode as the reference electrode and a monolayer-based gold electrode (0.09 cm^2) as the working electrode was employed. Prior to use, the flat gold electrode was polished, cleaned by sonicating and then pretreated electrochemically. The monolayer of TP on the gold electrode surface was prepared by immersing the electrode into 5×10^{-3} mol/L TP alcohol solution for about 30 min. The cyclic voltammetry was performed in 0.1 mol/L H_2SO_4 or in 5×10^{-3} mol/L $K_4Fe(CN)_6$/0.5 mol/L KCl. A.C. impedance measurements were performed in the solution of 5×10^{-3} mol/L $K_4Fe(CN)_6$/5×10^{-3} mol/L $K_3Fe(CN)_6$. After deaeration with pure N_2 for 30 min, all the electrochemical experiments were carried out at (25 ± 0.1)℃ inside a Faraday cage under N_2 atmosphere.

2 Results and discussion

2.1 The spectroscopic characterization of TP monolayer

The RA-FTIR spectra of TP monolayer modified gold electrode, at which the stretching band of Ar-H is at ca. 3 046 cm^{-1}, the skeletal vibration of the benzene nucleus at ca. 1 580, 1 480 and 1 440 cm^{-1}, and the bend band of C-S at ca. 1 100 and 1 030 cm^{-1}, indicate that the TP have formed the molecular layer at the gold electrode surface.

2.2 Determination of surface coverage (θ) of the TP monolayer

The total fraction of TP covered area at Au/TP electrode was determined quantitatively by means of the cyclic voltammetry in 0.1 mol/L H_2SO_4. Fig. 1 shows the typical cyclic voltammograms for various immersing time of gold electrode in TP solution. The redox peaks of the cyclic voltammograms correspond to the gold oxide formation and its removal. Comparison of the behaviour of bare gold with the monolayer covered electrode shows that the reduction currents of the gold oxide decrease markedly with the increase of the immersing time in TP solution. The quantity of gold oxide formed and hence the electrical charge consumed when its removal was proportional to the effective electrode area. As covered by TP, the effective electrode area decreases. The area under the reduction peak of oxide is assumed as a measure of the total fraction of uncovered area $(1-\theta)$, θ being the fraction of monolayer coverage. Therefore, comparison of the charge passing through under the reduction wave at Au/TP electrode with those at a bare electrode may serve as a measure of the electrode coverage of TP monolayer, i.e. $\theta=1-Q/Q_0$, where Q and Q_0 are

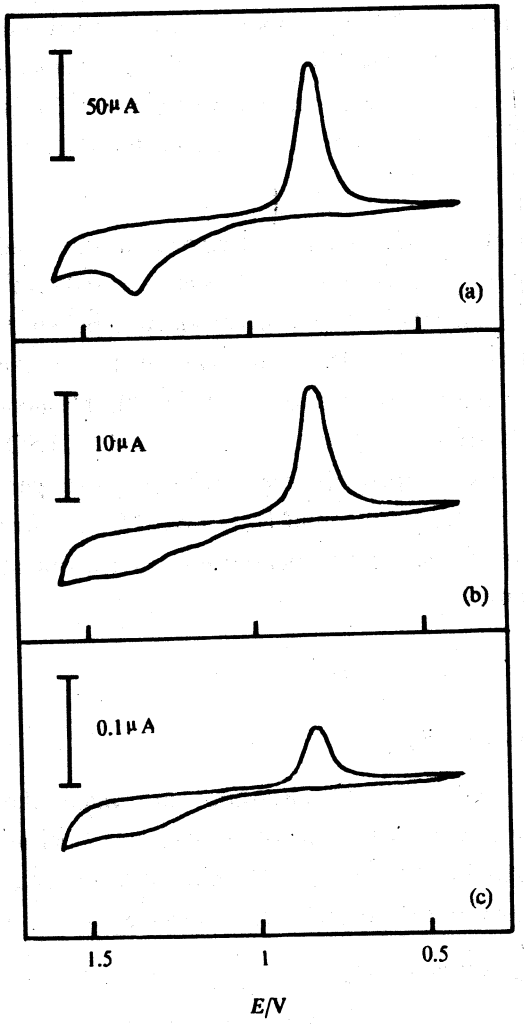

Fig. 1. Cyclic voltammograms in 0.1 mol/L H_2SO_4 (scan rate, 50 mV/s) for Au/TP electrode with θ values of (a) 0.00; (b) 0.83; (c) 0.999.

the reduction charge of gold oxide on TP-covered and bare gold electrodes, respectively. Fig. 1 indicates that the effective electrode area of the gold electrode immersed in TP solution for 15 and 60 min is only 17% and 0.1% that of bare gold electrode.

2.3 Cyclic voltammetric characteristics of Au/TP electrode

In order to gain a better insight into the detailed information of TP monolayer modified gold electrode, cyclic voltammetric experiments with $Fe(CN)_6^{4-}$ were performed with different coverage of θ and at various scan rates. A series of results are shown in fig. 2 and the peak current i_{pa} and the separation of peaks ΔE_p are summarized in table 1. As seen in fig. 2 and table 1, when the surface coverage $\theta \leqslant 0.83$, very small decrease, if any, in peak current is observed at moderate scan rates. With the increase of the coverage a moderate peak current diminution occurs, but even with $\theta = 0.999$ i.e. only 0.1% of the electrode area is active, the peak current i_{pa} can still remain 56% that at the bare gold electrode. At the same time, the separation of peaks (ΔE_p) increases substantially with the increase of the surface coverage, indicating a decrease in the apparent heterogeneous electron transfer rate constant.

Table 1 Voltammetric results summarized for the electrodes in fig. 2

θ	25 mV/s		50 mV/s		100 mV/s	
	i_{pa}	ΔE_p/mV	i_{pa}	ΔE_p/mV	i_{pa}	ΔE_p/mV
0.00	1.00	65	1.00	67	1.00	68
0.83	0.94	79	0.91	124	0.86	132
0.999	0.56	320	0.51	340	0.45	380

It was already shown by Amatore *et al.*[2] that under certain conditions the partially blocked electrode behaves as a microelectrode assembly and an electrode reaction at a

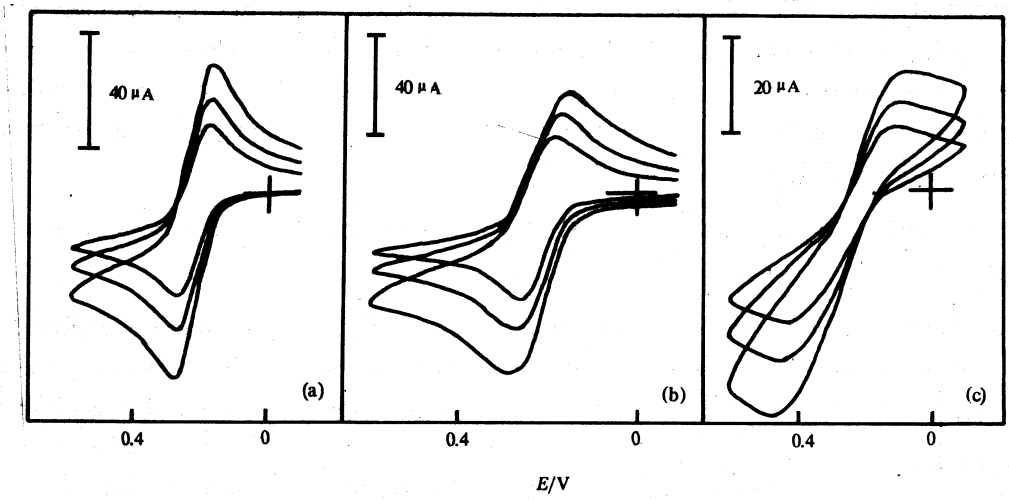

Fig. 2. Cyclic voltammograms for 5×10^{-3} mol/L $Fe(CN)_6^{4-}$ in 0.5 mol/L KCl aqueous (scan rate, 25, 50, 100 mV/s) at Au/TP electrode with θ values of (a) 0.00; (b) 0.83; (c) 0.999.

microelectrode assembly would appear to be kinetically slower than that at a macroelectrode. For partially blocked Au/TP electrode, every active site uncovered by TP can be taken as a microelectrode; namely, Au/TP is a microelectrode assembly. Consequently, the apparent heterogeneous electron transfer rate constant k_{app} of $Fe(CN)_6^{4-}$ at Au/TP monolayer based microelectrode assembly decreases with the increase of the surface coverage of TP. At low scan rate, the time domain of the experiment is relatively long; the thickness of diffusion layer at every microelectrode is larger than the distance between the two adjacent microelectrodes; the individual spherical diffusion layers overlap; thus, a semiinfinite linear diffusion similar to macroelectrode type behaviour would be expected, corresponding to the entire geometric area of gold electrode. At moderate scan rate, the thickness of diffusion layer is not so large compared to the microelectrode diameter but still smaller than the distance between two adjacent microelectrodes; a microelectrode-type behaviour occurred as spherical diffusion to individual microelectrode. At fast scan rate, the diffusion layer thickness is very small in comparison with the microelectrode diameter; a semiinfinite linear diffusion is again expected as the same as that at macroelectrode, in this case corresponding to the cumulative area of the individual microelectrodes. The cyclic voltammograms in fig. 2 show the characteristics of microelectrode assembly.

An outstanding property of the monolayer-based microelectrode assembly is the different voltammetric behaviour exhibited at moderate scan rate for the electrochemical reaction controlled by diffusion compared to surface reaction at the same electrode. Thus, with an electrode of, say, $\theta=0.999$, peak current originating from surface reaction (such as gold oxide formation/removal) will reduce to 0.1% (as seen in fig. 1), whereas the peak current corresponding to the reaction controlled by diffusion will remain 56% that at the

bare gold electrode. The characteristics of monolayer-based microelectrode assembly can be used to achieve substantial signal-to-noise improvement in certain electrochemical experiments. For example, when an electrochemical reaction contains both the surface and diffusion process, the monolayer-based microelectrode assembly can suppress the surface process effectively and facilitate the diffusion process.

2.4 A.C. impedance characteristics and the determination of large heterogeneous rate constant

As discussed above (see fig. 2 and table 1), an important phenomenon expected for monolayer-based microelectrode assembly under appropriate conditions is an apparent decrease in the value of the heterogeneous electron transfer rate. This provides, in principle, the possibility of "slowing down" a rapid electrode reaction to the extent that it can be conveniently studied, provided that the "real" rate constant can be calculated from the apparent one. As is shown below, this decrease is directly proportional to the fraction of active surface $(1-\theta)$. Fig. 3 presents complex impedance plots for $Fe(CN)_6^{4-/3-}$ redox couple, measured with a bare gold and Au/TP electrode at various θ values. The semicircle in the higher frequency and the line at lower frequency correspond to the charge transfer impedance and the Warburg impedance, respectively. It can be seen from fig. 3(a) that no kinetic information can be obtained with a bare gold electrode under those conditions. The charge transfer resistance R_{ct}, measured as the diameter of the semicircle in the higher frequency, increases with the increase of the surface coverage θ of TP indicating an apparent decrease in the rate of the heterogeneous electron transfer step.

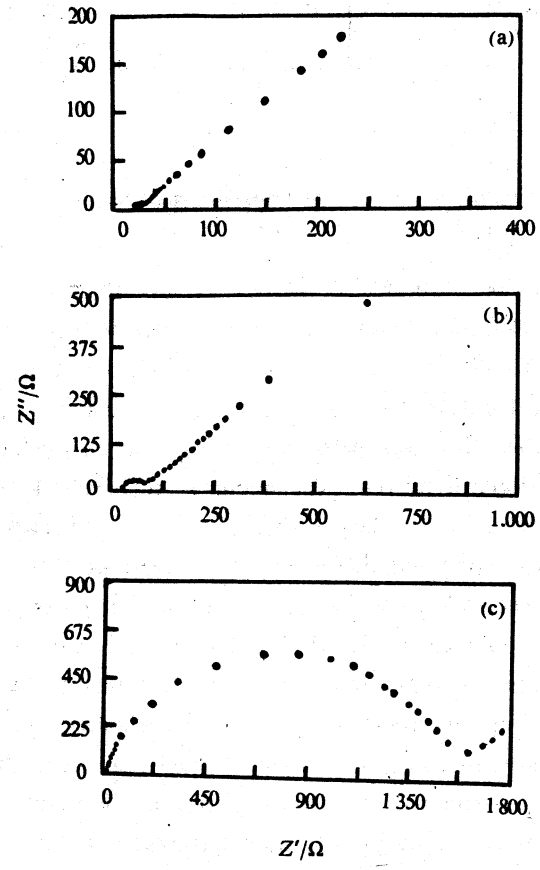

Fig. 3. Complex impedance plots for 5×10^{-3} mol/L $Fe(CN)_6^{4-}$ $+5\times10^{-3}$ mol/L $Fe(CN)_6^{3-}$ in 0.5 mol/L KCl at Au/TP electrode with $1-\theta$ values of (a) 1.00; (b) 0.17; (c) 0.001.

Within the time domain where a kinetic semicircle is observed in the complex impedance plot, the elctrode reaction is kinetically controlled by the electron transfer. Thus the following simple relationships hold for a one-electron transfer in the first-order reaction

with $c_{ox}=c_{red}=c$,

$$R_{ct}=\frac{1}{i_0}\cdot\frac{RT}{F}, \tag{1}$$

$$i_0=Fk_{app}c \tag{2}$$

and

$$k_{app}=k^0(1-\theta), \tag{3}$$

where i_0 is the exchange current, k^0 the heterogeneous standard rate constant, c the concentration of $Fe(CN)_6^{4-/3-}$. Thus, k_{app} and also k^0 can be calculated from the above equations. The results are listed in table 2. The average value of k^0 for $Fe(CN)_6^{4-/3-}$ is 0.037 cm/s, which is in good agreement with that obtained by Oyama[3] using fast scan cyclic voltammetry (0.06 ± 0.05 cm/s).

Table 2 The measurements of A.C. impedance results for the Au/TP electrode in fig. 3

$1-\theta$	R_{ct}/Ω	$k_{app}\times10^5/cm\cdot s^{-1}$	$k^0\times10^2/cm\cdot s^{-1}$
0.17	80.2	674	3.96
0.001	1553.8	3.42	3.42

References

1 Chidsey, C. E. D., Bertozzi, C. R., Putvinski, T. M. *et al.*, Coadsorption of ferrocene-terminated and unsubstituted alkanethiols on gold: electroactive self-assembled monolayer, *J. Am. Chem. Soc.*, 1990, 112: 4301.

2 Amatore, C., Saveant, J. M., Tessier, D. *et al.*, Charger transfer at partially blocked surfaces: a model for the case of microscopic active and inactive sites, *J. Electroanal. Chem.*, 1983, 147: 39.

3 Oyama, N., Ohsaka, T., Yamamoto, N. *et al.*, Determination of the heterogeneous electron-transfer rate constant for the redox couples $Mo(CN)_8^{4-/3-}$, $W(CN)_8^{4-/3-}$, $Fe(CN)_6^{4-/3-}$, $Os(CN)_6^{4-/3-}$, and $IrCl_6^{3-/2-}$ using fast sweep cyclic voltammetry at carbon fibre electrodes, *J. Electroanal. Chem.*, 1989, 265: 297.